agriculture

Article

Analysis and Optimization Test of the Peanut Seeding Process with an Air-Suction Roller Dibbler

Yang Xiang [1,2], Jianming Kang [1,3,4,*], Chunyan Zhang [1,3], Qiangji Peng [1,3], Ningning Zhang [1,3] and Xiaoyu Wang [1,3]

1 Shandong Academy of Agricultural Machinery Sciences, Jinan 250100, China
2 School of Agricultural Engineering and Food Science, Shandong University of Technology, Zibo 255000, China
3 Huang Huai Hai Key Laboratory of Modern Agricultural Equipment, Ministry of Agriculture and Rural Affairs, Jinan 250100, China
4 Shandong Academy of Agricultural Sciences, Jinan 250100, China
* Correspondence: kangjianming@shandong.cn

Abstract: The air-suction roller dibbler for peanuts is the core component to realizing precision seeding on film; however, the seeds in the dibbler cannot accurately fall into the seed-guiding mechanism during the work. In this study, we stabilized the seed trajectory by adjusting the installation angles of the chock block (IACB) and installation angles of the dibbler cover (IADC). We studied the seed-movement characteristics under different IACB and dibbler covers using EDEM simulation software. The separation between the seed and the baffle was obtained for different installation conditions, which were contact separation and noncontact separation. We obtained the best seeding performance when the seed was released from the edge of the dibbler cover in contact with the baffle of the seed separation tray. In the bench test, we obtained the best seed-feeding performance at 48.28° for the IACB, 12.29° for the IADC, and 3.84 km/h for the machine. The seeding pass rate was 95.35%, the missed seeding rate was 2.52%, and the reseeding rate was 2.11%. The field verification test showed that the machine worked well with the combination, and the seeding pass rate was above 92%, which meets the requirements of the single-grain precision sowing of peanuts and substantially improves the operation performance.

Keywords: peanut; air-suction roller dibbler; seed-feeding-delivery performance; parameter optimization

Citation: Xiang, Y.; Kang, J.; Zhang, C.; Peng, Q.; Zhang, N.; Wang, X. Analysis and Optimization Test of the Peanut Seeding Process with an Air-Suction Roller Dibbler. *Agriculture* **2022**, *12*, 1942. https://doi.org/10.3390/agriculture12111942

Academic Editor: John M. Fielke

Received: 25 October 2022
Accepted: 16 November 2022
Published: 17 November 2022

1. Introduction

The peanut is a major economic and oilseed crop in China, ranking first in the world in total production and export, with a planting area of about 4.6 million mu, and a total production of about 17 million tons [1]. The film mulching system is an important way to grow peanuts in China. This planting method has the effect of increasing the temperature and moisture retention, which not only shortens the growth cycle of peanuts but also increases the fruit yield [2].

The single-grain planting of peanuts alleviates the competition between adjacent plants, gives fuller play to the production potential of a single plant, and improves the yield; however, the sowing accuracy has been a difficult problem in single-grain mechanized seeding [3]. The air-suction roller dibbler has the characteristics of single-grain seed extraction, but there are phenomena such as omission and reseeding in the actual operation, which directly affect the sowing effect [4,5].

Ensuring the accurate seed feeding of the seed-discharge mechanism is an important prerequisite for high-speed precision-seeding operations. Many scholars have conducted extensive research on the seed-discharge performance of seed dischargers in recent years [6,7]. Liao et al. [8–11] used a high-speed camera and image-target-tracking technology to analyze the seed-feeding trajectory of a seed rower, and they derived the seed-feeding-trajectory curve. A precision seeding equipment (John Deere, Moran, IL, USA), set the seed-guide tube of the no-till planter into an inclined curve structure. They equipped the inner side of the seed-guide tube with a photoelectric sensing system to synchronously detect reseeding and omission [12]. Kocher [13] compared and analyzed the variation in the seed-pitch uniformity of seeds of different shapes under different seed guides, with the smoothness of the inner wall of the seed guide as the test factor. Ding et al. [14] analyzed the influence of the seed-adsorption attitude on the seeding performance by simulating the seeding process of the seed rower with the help of the DEM–CFD coupling method. Wang et al. [15] used airflow-assisted seed dropping and introduced positive airflow into the seed-guide tube to promote rapid seed dropping and reduce collisions with the tube wall to ensure the uniformity of the grain spacing. Lv et al. [16] added a reverse-acceleration device to make seed potatoes drop under the action of gravity and the positive pressure of blowing seed, which improved the stability of the seed dropping. Gao et al. [17,18] combined the forward machine speed of the machine to set the location of the seed-dropping point to realize the zero-speed seed-dropping of the seed-row mechanism. Li et al. [19] designed a vertical conduit suitable for the straight and stable movement of seeds by studying the trajectory of the seeds in the seed tray and a seed-pushing device. Chen et al. [20,21] designed a belt-type seed-guide device in which the seeds were escorted to the seeding point by belt paddles, which reduced the seeding height and ensured the uniformity of the rows of the seed grain spacing. Zhang et al. [22] added a secondary seeding mechanism between the duckbill and seed tray of the air-suction roller dibbler. They determined parameters such as the installation position, seed-channel profile, and structure of the entrance and exit. However, researchers have mainly conducted such studies to improve the seed-delivery performance by optimizing the structure of the seed-guide mechanism or improving the seed-delivery method [23,24]. The smoothness of the seed entry from the seed chamber into the seed-guiding mechanism is also particularly critical. If the seeds are thrown out at a certain initial speed at the seed suction tray, they are affected by the collision and start to enter the seed-guiding mechanism after bouncing and tumbling along the edge of the dibbler cover. Due to the collision between the seed and the seed separation tray in the process of falling, the seed which has obtained a certain acceleration does not fall into the corresponding area of the seed channel accurately, then it is prone to omission, reseeding, and reduced sowing accuracy.

In this study, we optimized the installation angles of the chock block and dibbler cover. We analyzed the mechanism of the change in the seeding trajectory of peanut seeds by establishing a kinematic model. We analyzed the law of the peanut-seed movement during seeding with the help of EDEM software to study the influence of the installation angle of the chock block (IACB) and the installation angle dibbler cover (IADC) on the seeding performance to improve the seeding performance of the air-suction roller dibbler.

2. Materials and Methods

2.1. Structure and Working Principle of Peanut Film Seeder

We used the double-row ridge planting method, with the following parameters: hole spacing: about 120–140 mm; sowing depth: about 30–50 mm.

We present the peanut mulching-and-seeding machine in Figure 1a. The main structure comprises a plowing device, suppression device, film-spreading device, covering device, seeding device, spraying device, and fertilizing device. These devices are coordinated and closely connected; the planter is connected to the tractor by three-point suspension. We present the structure of the planter seeding device in Figure 1b. The pulley drives the blower to provide a negative-air-pressure environment in the seed-extraction chamber of the dibbler. While the machine is moving forward, the soil is first plowed and passed through a suppression roller to form a trapezoidal ridge belt. The motor provides power to drive the fertilizer discharger to rotate in the fertilizer-application device. The fertilizer is discharged from the end of the furrow opener along the fertilizer-guide tube, and the spraying device then carries out the drug spraying. In the mulching process, the mechanism spreads the film on the ridge. The film press wheel fixes the film so that the small mulching disc mulches the film edge for the first time. The dibbler rotates with the advance of the unit to realize the seeding on the film, and then the large mulching disc performs the second mulching.

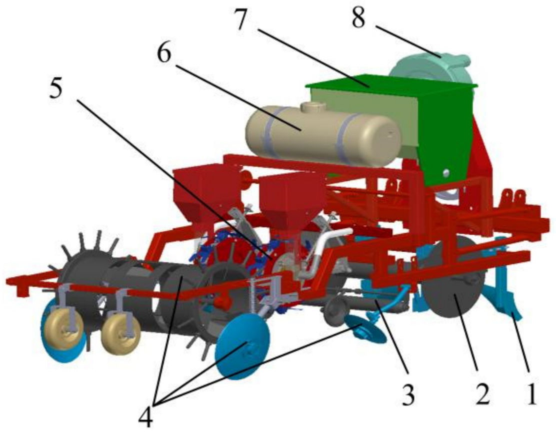

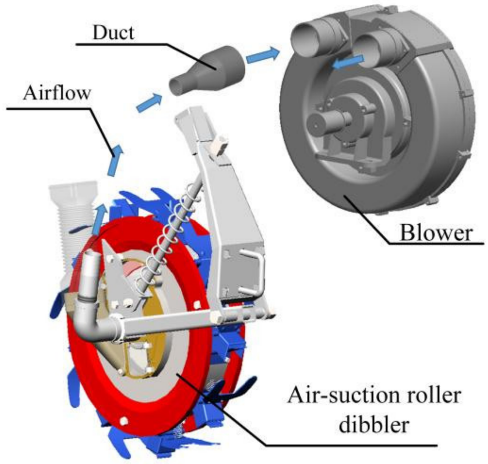

Figure 1. (**a**) Schematic diagram of film precision peanut seeder: (1) plough; (2) suppression roller; (3) film-spreading device; (4) mulching device; (5) seeding device; (6) spraying device; (7) fertilizer-application device; (8) blower; (**b**) structure of seeding device.

2.2. Structure and Working Principle of Dibbler

We present the specific structure of the air-suction roller dibbler for peanuts, which is mainly composed of a seed-delivery tube, side plate, seed separation tray, seed-guiding mechanism, belt, chock block, dibbler shaft, duckbill, seed suction tray, and dibbler cover, in Figure 2. The working process of the dibbler mainly includes four stages: seed taking, seed cleaning, seed carrying, and seed feeding. When the machine is working, the blower provides negative airflow, which passes through the dibbler shaft to form a negative pressure in the seed chamber so that the peanut seeds are stably adsorbed on the suction-tray hole. The suction tray rotates with the advance of the machine, and the seed-cleaning brush removes the excess seeds in the seed-cleaning area. The seeds are adsorbed on the seed suction tray in a circular motion. When the adsorbed seeds pass through the chock block, the seeds enter the seed drop zone and leave the seed suction tray under gravity. During the seed-feeding process, the seed baffle and the cover limit the vertical and horizontal movement of the seeds to a certain extent. Subsequently, the seeds are pushed by the baffle to the exit of the cover, and fall into the seed guide mechanism. The seed-guiding mechanism acts as a transition device to make the seeds steadily fall into the duckbill. The duckbill breaks the film into the soil, and the seeds finally enter the cavity.

The suction tray is a key component of the air-suction roller dibbler. The seeds are transported in the dibbler mainly by the suction tray, which adsorbs the seeds and synchronously rotates. Its diameter size determines the size of the dibbler, the number of holes, and other important parameters. To ensure that the suction tray could effectively take the seeds, we analyzed the relationship between the processes of taking seeds and carrying seeds for the suction tray:

$$\begin{cases} t_1 = \frac{C_r}{v_p} \\ C_r = \alpha\left(r_p - r_k\right) \\ v_p = \frac{\pi n}{30}\left(r_p - r_k\right) \end{cases} \tag{1}$$

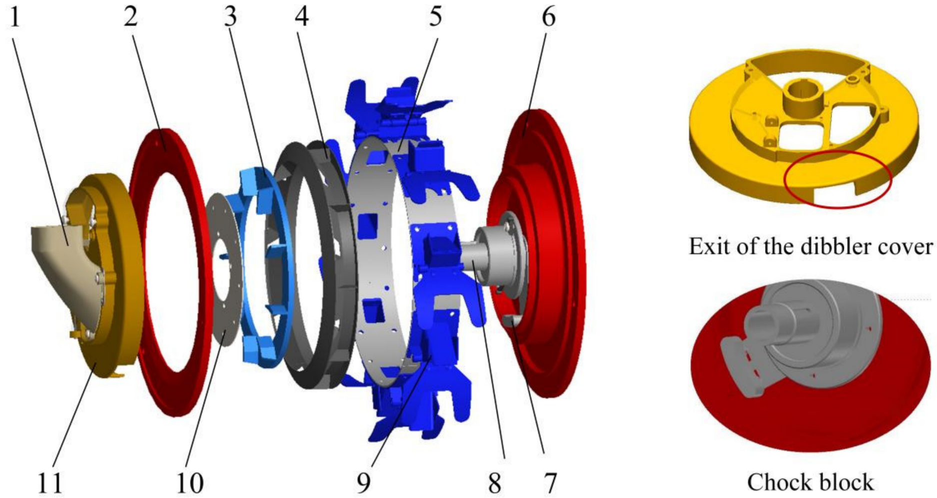

Figure 2. Internal structure diagram of dibbler: (1) seed-delivery tube; (2) side plate 1; (3) seed separation tray; (4) seed-guiding mechanism; (5) belt; (6) side plate 2; (7) chock block; (8) dibbler shaft; (9) duckbill; (10) seed suction tray; (11) dibbler cover.

2.3. Key-Parameter Selection and Seed-Feeding-Process Analysis

2.3.1. Selection of Key Parameters for Dibbler

From Equation (1), we can obtain:

$$t_1 = \frac{30\alpha}{\pi n} \tag{2}$$

where t_1 is the time that the seed is in the seed-absorbing zone (s); C_r is the arc length of the seed-taking zone (m); v_p is the linear velocity of the seed suction tray (m·s^{-1}); α is the angle of rotation of the seed-taking zone (rad); r_p is the radius of the seed suction tray (m); n is the rotational speed of the seed suction tray (r·min^{-1}); r_k is the radial distance between the center of the hole and the edge of the seed suction tray (m).

According to Equation (2), the seed-taking time of the seed suction tray is related to the angle of the rotation of the seed-taking zone and the rotational speed of the seed suction tray, and is not related to the radius of the seed suction tray. The radius of the seed suction tray of the seeding device is generally 40–130 mm [25], and in this study, the diameter of the seed suction tray was 100 mm. According to the design structure of the dibbler, the parameter relationships are satisfied as follows:

$$\begin{cases} vT = lN \\ N = \frac{znT}{60} \\ \alpha_T = \frac{360^\circ}{N} \end{cases} \tag{3}$$

where v is the forward speed of the unit (m·s^{-1}); T is the operating time of the planter (s); l is the peanut spacing (mm); N is the number of seed grains per circle; z is the number of seed-suction tray holes; α_T is the center angle of the two adjacent holes (°).

According to the n, v, and l, the number of seed-suction tray holes (z) is 9, and the center angle of the adjacent holes (α_T) is 40°. We present the internal structural parameters of the dibbler in Figure 3a: the distance from the center of the seed-suction tray hole to the center of rotation is 82 mm; the radius of the seed separation tray is 128 mm; the diameter of the seed-guiding mechanism is 320 mm; the height of the seed channel is 25 mm; the interval of the baffle inside the seed-guiding mechanism is 40°; the radius of the dibbler side plate is 184 mm. We present the seeding trajectory under different installation angles of the chock block in Figure 3b. As the installation angle of the chock block changes, the seeds that fall to the edge of the dibbler cover are shifted. Assuming that the seeds fall to the edge of the cover at the lowest point, we can obtain:

$$\begin{cases} \omega r_k t_2 \cos\theta = r_k \sin\theta \\ \omega r_k t_2 \sin\theta + g{t_2}^2 = R - r_k \cos\theta \end{cases} \tag{4}$$

where θ is the angle between the line between the feeding point and the center of rotation and the normal; g is the acceleration of the gravity (m·s^{-2}); t_2 is the time of seed drop to cover (s); and R is the seed separation tray radius (mm).

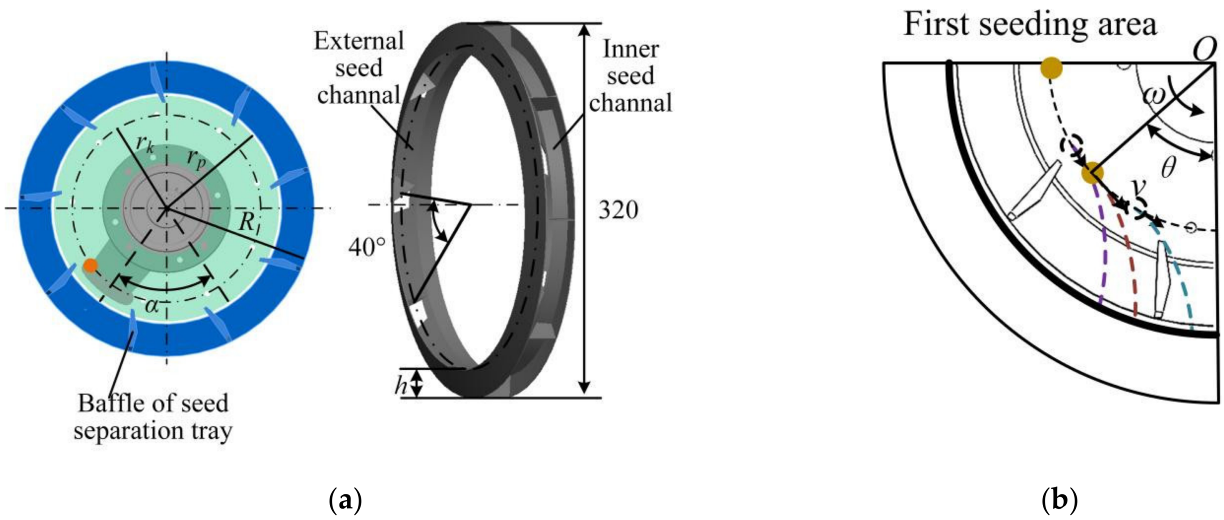

Figure 3. (**a**) Internal structural parameters of the dibbler; (**b**) seed-feeding trajectory at different chock-block installation angles.

Thus, the IACB directly affects the seeds' seeding trajectory and contact state with the seed separation tray and dibbler cover. The common IACB for air-suction dibblers ranges from 30° to 60°.

2.3.2. Analysis of Seed-Feeding Process

When the peanut seeds enter the seed-guiding mechanism, it is mainly in two forms. The seeds leaving the dibbler cover in contact with the baffle of the seed separation tray Figure 4a is the most common form in the seed-feeding process. We present a depiction of the seed leaving the dibbler cover in a noncontact state with the baffle of the seed separation tray in Figure 4b. At this time, the seed-velocity direction is more complicated, making it difficult to maintain stability. This is because the seeds are not subjected to the continuous thrust of the seed separation tray, which makes it difficult for them to maintain a constant circular motion along the edge of the cover.

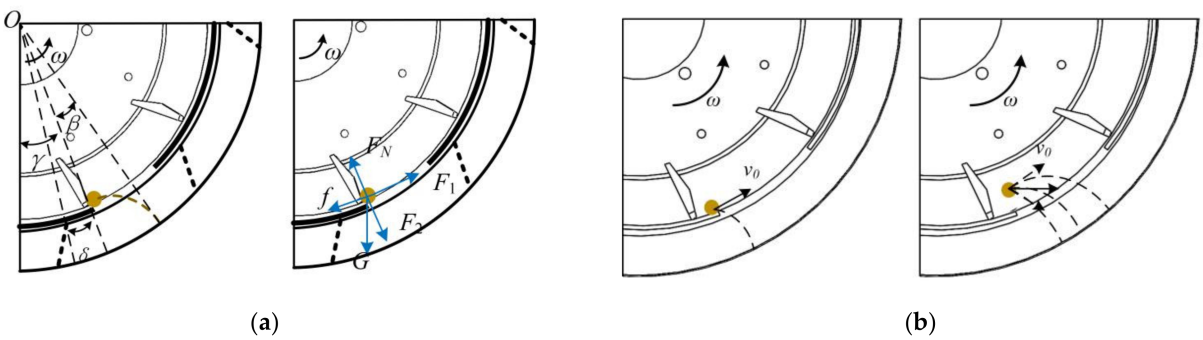

Figure 4. Two forms of leaving the dibbler cover: (**a**) contact; (**b**) noncontact.

The trajectory of the seed separation from the dibbler-cover phase is generally similar in the contact-separation mode, and the initial position of the seed separation is the lowest throwing point. The direction of the seed movement is perpendicular to the line between the lower edge of the dibbler-cover opening and the center of rotation. γ is the installation angle of the dibbler cover (the angle between the initial velocity and horizontal direction), and the initial velocity (v_0) is approximately equal to the linear velocity of the edge of the seed separation tray:

$$v_0 = \omega R \tag{5}$$

where ω is the angular velocity of the seed dispenser (rad·s^{-1}).

The seeds are in uniform linear motion in the horizontal direction when the seeds are thrown and in the vertical direction to perform the free-fall motion. The time required for the seed to drop from the edge of the opening of the dibbler cover to the seed-guiding mechanism is t_3. Ignoring the radius of the seed, the horizontal and vertical directions of the motion-trajectory equation are as follows:

$$\begin{cases} x = \omega R t_3 \cos\gamma \\ y = \frac{1}{2} g t_3^2 - \omega R t_3 \sin\gamma \end{cases} \tag{6}$$

where x is the horizontal displacement in time (t_3) (mm); y is the vertical displacement in time (t_3) (mm).

After the seed touches the wall of the seed channel of the seed-guiding mechanism, the separation is completed. The height of the seed channel of the seed-guiding mechanism is h. The rotation angle of the dibbler is the minimum angle (β) required during the seed separation from the dibbler-cover phase when the seed directly falls to the bottom of the seed channel:

$$x + R\sin\gamma = (R + h)\sin(\gamma + \beta) \tag{7}$$

The number of duckbills in the dibbler is nine, and the angle between the adjacent baffles in the seed channel is 40°. In order to avoid the seeds colliding with the baffles, the seed-guiding-mechanism installation angle (δ) needs to meet the following relationship:

$$\delta \leq 40^\circ - \arcsin\left(\frac{\omega R t_2 \cos\gamma + R\sin\gamma}{R + h}\right) + \gamma \tag{8}$$

From Equation (8), the seed-guiding-mechanism mounting angle is related to the dibbler speed and dibbler-cover mounting angle when the height of the seed channel of the seed-guiding mechanism and the diameter of the seed separation tray are determined. To avoid the interference of the top part of the baffles, we selected 10° for the δ. According to the preliminary test, the seed-feeding trajectory is more stable in the range of [5°, 20°] for the dibbler-cover mounting angle.

To study the law of the seed movement in the initial stage of the seed leaving the dibbler cover and to determine the contact state between the seed and the baffle of the seed separation tray, we performed a mechanical analysis of the seeds that were detached from the edge of the dibbler cover. The equation of the equilibrium of the forces on the seeds is as follows:

$$\begin{cases} F_N - F_2 - G\cos\gamma = 0 \\ F_1 - G\sin\gamma - f = 0 \\ F_2 = m\omega R \\ f = \mu F_N \end{cases} \tag{9}$$

where F_1 is the thrust force of the baffle on the seed (N); F_N is the support force of the seed by the cover (N); F_2 is the centrifugal force on the seed (N); G is the gravity of a single peanut seed (N); f is the friction force of the cover on the seed (N); μ is the coefficient of the friction between the dibbler cover and seed.

From Equation (9), we obtain:

$$F_1 = \mu m\omega R + mg(\mu\cos\gamma + \sin\gamma) \tag{10}$$

According to Equation (9), the thrust force of the baffle of the seed separation tray on the seed is determined by the γ under the condition that the radius of the seed separation tray is determined, and the thrust force of the baffle of the seed separation tray on the seed gradually increases with the decrease in the γ. In the initial stage of seed-cover separation, the contact between the seeds and the baffle of the seed separation tray depends on the force between them. When F_1 = 0, the seeds are separated in a noncontact manner; when F_1 > 0, the seeds are separated in a contact manner. The greater the interaction force between the seeds and the baffle of the seed separation tray, the easier it is for them to maintain contact. The seeds can smoothly enter the seed-guiding mechanism in their separation from the dibbler-cover phase and continue to move along the seed channel to determine whether the seed delivery is qualified. Thus, the separation mode directly affects the seed-delivery performance of the dibbler.

In the noncontact separation process, the collision between the seed and the baffle is the main reason to reduce the seeding performance; on the contrary, when the seed is separated from the cover by contact separation, its initial velocity direction and magnitude are basically the same, and the trajectory is more stable. The vibration caused by unstable ground conditions during field operation increases the number of noncontact separations. To achieve the goal of a stable seeding trajectory and reduced noncontact separations, we need to start with the impact of the IACB and IADC on the separation.

2.3.3. Simulation Test

In order to derive the influences of the IACB and IADC on the trajectory of the seed-feeding process, we selected EDEM simulation software (DEM Solutions Limited, Edinburgh, UK) for the simulation analysis. We selected the peanut seeds from HuaYu 25 (SAAS, Jinan, China). We measured the average lengths and circumferences of the 100 seeds at 14.44 and 8.99 mm, respectively. We built the peanut-seed model, dibbler model, and seed-collection box in SOLIDWORKS software (Dassault Systemes S.A, Waltham, MA, USA). We imported the model into EDEM software in the STEP format and built a particle factory inside the dibbler model. We present the models in Figure 5.

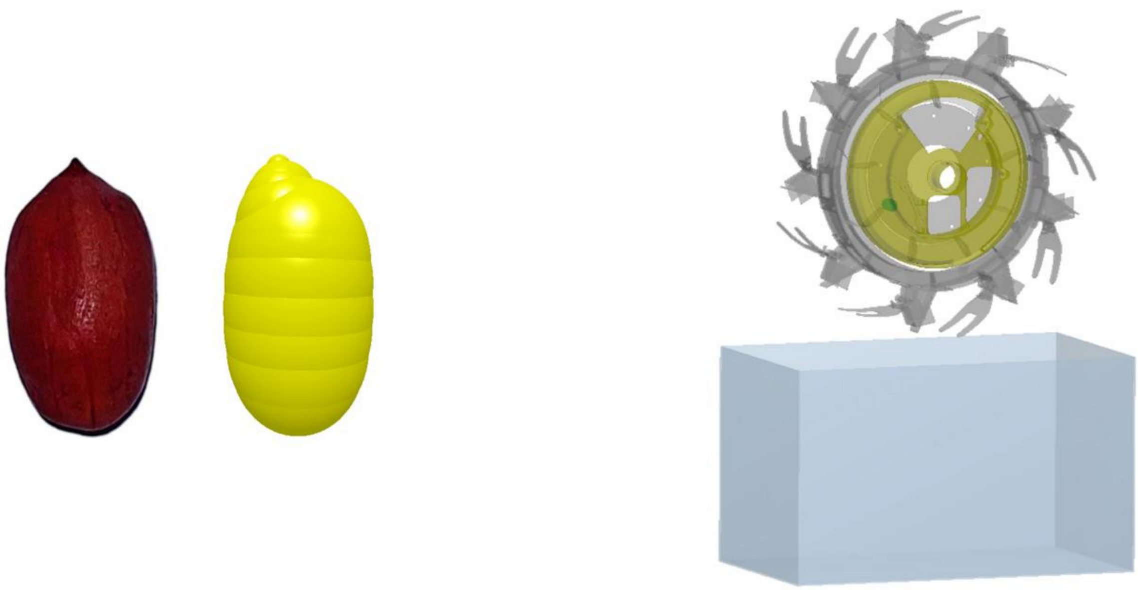

(**a**) (**b**)

Figure 5. Simulation models: (**a**) seed model; (**b**) dibbler model.

Considering the smooth and nonadhesive peanut seed surface, the Hertz–Mindlin contact model was used for the simulation tests. The seed and material parameters and seed-material contact parameters were set with reference to the literature [26]. We set the simulation parameters as shown in Table 1. When the machine's forward speed is 4 km·h^{-1}, the rotation speed of the dibbler is 0.88 r·s^{-1}, and the initial velocity of the seed-feeding point is 0.45 m·s^{-1}. The velocity direction is perpendicular to the line connecting the center of the particle factory and the center of rotation. The number of seeds per lap of the dibbler is nine, and so the number of seeds generated per second in the pellet plant is 7.95. Finally, we set the fixed time step to 7.3×10^{-6} s.

Table 1. Simulation parameter settings.

Project	Parameter	Numerical Value
Peanut properties	Poisson's ratio	0.362
	Density (kg·m^{-3})	1.04×10^3
	Shear modulus (Pa)	5.06×10^7
Attributes of seed-guide mechanism	Poisson's ratio	0.394
	Density (kg·m^{-3})	2.05×10^3
	Shear modulus (Pa)	7.9×10^8
Coefficient of restitution	Seed–seed	0.501
	Seed–seed guide mechanism	0.500
Coefficient of static friction	Seed–seed	0.213
	Seed–seed guide mechanism	0.300
Coefficient of rolling friction	Seed–seed	0.035
	Seed–seed guide mechanism	0.030
Other parameters	Gravitational acceleration (m·s^{-2})	9.81

2.3.4. Bench Test and Evaluation Methods

In order to analyze the factors that affect the seeding pass rate, we established the following bench test. The bench test was designed as an orthogonal experiment based on the Box–Benhnken test design principle. We tested a sample of one hundred peanut seeds with a mass of 61.3 g and a mass moisture content of 13.15%. We conducted the test to study the seed-feeding performance of the dibbler by using the IACB and IADC, and the forward speed as the factors, setting the forward speed of the dibbler to 3–5 km·h^{-1}, according to the seeder operation, setting the IACB to 30°–60°, according to the installation parameters of the dibbler, and setting the IADC to 10°–20°. We present the codes in Table 2, in which the codes X_1, X_2, and X_3 represent the IACB, IADC, and forward speed, respectively.

Table 2. Test factor levels.

Code	X_1 (°)	X_2 (°)	X_3 (km·h^{-1})
−1	30	10	3
0	45	15	4
+1	60	20	5

We present the seeding bench test in Figure 6, located at the Huang Huai Hai Key Laboratory of Modern Agricultural Equipment, the Ministry of Agriculture and Rural Affairs. We recorded the number of seeds passing through the sensor-monitoring area, where we installed an infrared alignment sensor at the exit of the dibbler cover. According to the GB/T 6973-2005 single-grain seeder test method [27], we designed 17 groups of experiments, and we used the seeding pass, missed seeding, and reseeding rates as the test indexes. We repeated each group of experiments three times to obtain the average values.

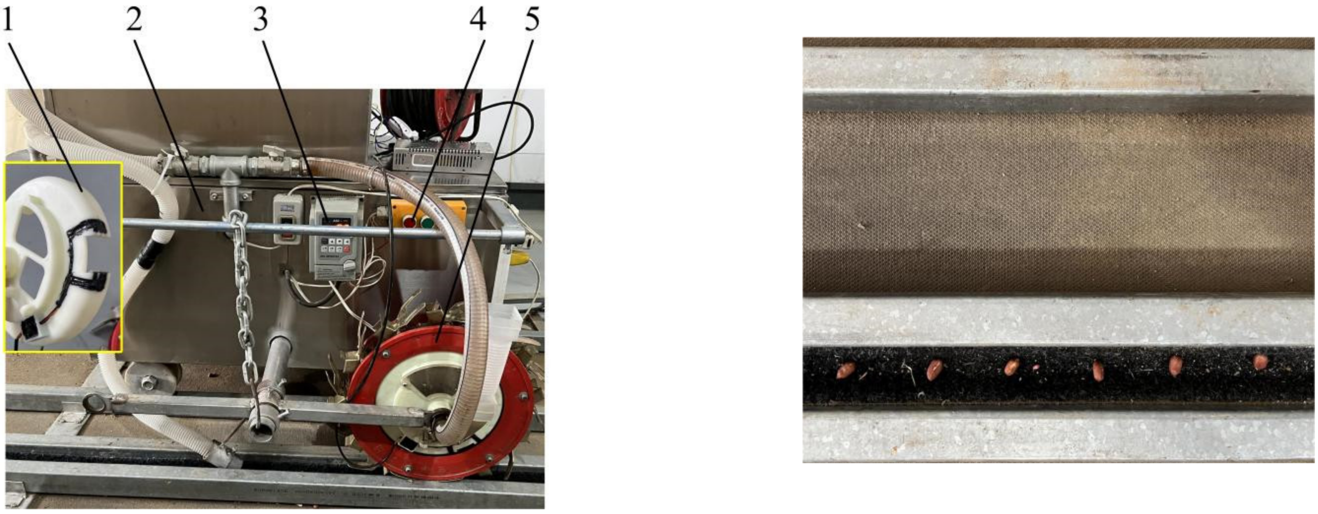

(**a**) (**b**)

Figure 6. (**a**) Seeding bench test: (1) infrared sensors; (2) pressure-supply device; (3) controller; (4) switch; (5) dibbler; (**b**) diagram of seeding effect.

2.3.5. Field Verification Trials

To further verify the reliability of the optimized installation combination, we used the optimal parameters obtained from the bench test to conduct field tests on the combination. The experiment was conducted in a flat test field with light sandy soil and a soil moisture content of 13% to 15%. We randomly examined the seeding of the machine tools within 5 m of 5 ridges after the operation with a meter ruler.

3. Results and Analysis

3.1. EDEM Simulation Results

3.1.1. Analysis of Seed-Feeding-Trajectory Principle

The seed state is displayed during the simulation in the Stream format, as shown in Figure 7a. The seed-movement area in the dibbler mainly includes the following: seed-feeding area; seed separation from the dibbler-cover area; transition area of seed channel III; duckbill seed-channel area IV. We present the velocity profiles of individual seeds, generated at 0.3 s, in Figure 7b. The velocity variation in area I is large because the seeds fall under the action of gravity, and the baffle of the seed separation tray and the dibbler cover limit the vertical and horizontal movements of the seeds to a certain extent during the falling process [28,29]. At 0.5–1.0 s, the seeds move to area II under the pushing action of the baffle of the seed separation tray and fall into the seed-guiding mechanism. The seeds complete the transition between the outer and inner seed channels of the seed-guiding mechanism in area III, during which the seed speed slowly changes.

3.1.2. Effect of IACB on Seed-Movement Speed

The change in the seed velocity during seeding can directly reflect the stability of the seed trajectory. We extracted the seed-velocity curves of the seeds in area I and area II under different IACB, and we chose three from each group, as shown in Figure 8. After the seeds fell to the edge of the dibbler cover, the baffle of the seed separation tray pushed the seeds forward. Because the horizontal force of the baffle of the seed separation tray on the seeds changes the velocity of the seeds in the *X*-axis direction, the change in the seed velocity in area II during the seeding process is mainly reflected in the *X*-axis direction.

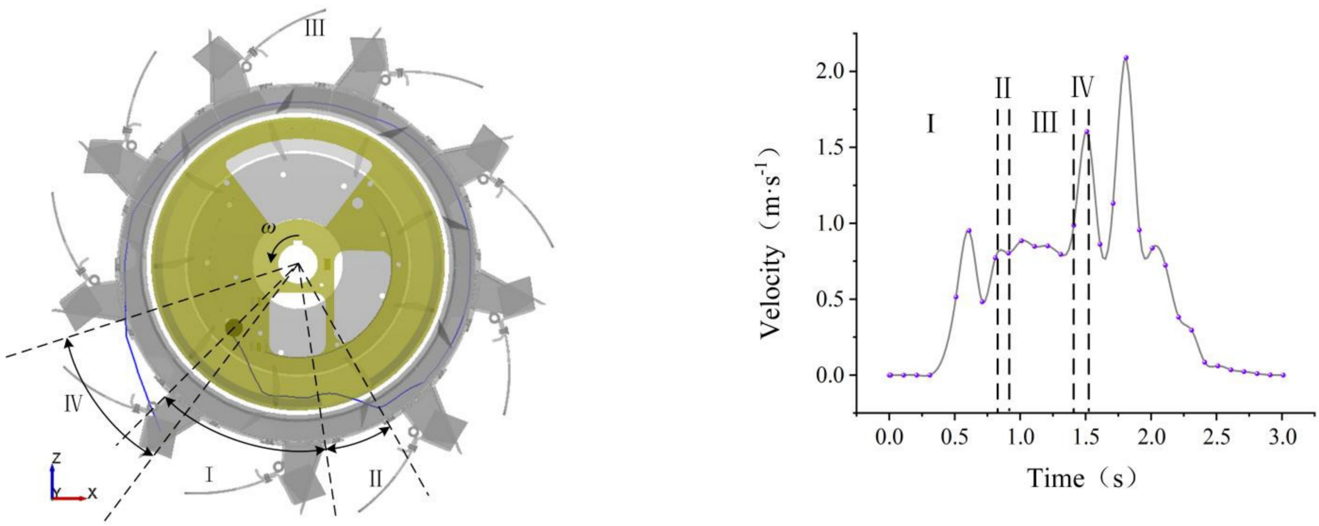

(**a**) (**b**)

Figure 7. (**a**) Seed-trajectory curve; (**b**) seed-velocity variation curve.

As shown in Figure 8, the velocity possessed by the seed when it first falls to the dibbler cover increases with the IACB increase, and the larger the IACB, the more obvious the velocity change when the seed moves at the edge of the cavity seeder cover when other factors are certain. The seed-velocity curves in area II mainly correspond to the curves within 0.20–0.35 s. According to the velocity curves Figure 8b,d,f in the *X*-axis direction, the seed velocity in the *X*-axis direction varies in different stages, and the seed separation from the dibbler-cover phase is slightly delayed with the IACB increase. When the IADC and speed of the dibbler are fixed, the velocity-variation interval when the seed leaves the cover decreases with the EACB increase, and the velocity-variation interval at the IACB of 60° is smaller than the other angles. As the seeds leave the cover with low kinetic energy, the horizontal displacement during the seed separation from the dibbler-cover phase is small, and it is easy for them to fall into the effective area of the seed-guiding mechanism. Thus, increasing the IACB can improve the stability of the trajectory.

As the IADC gradually increases, the seed drop time is delayed, and the kinetic energy of the seed at the initial point is gradually reduced. When the seed is separated from the cover with lower kinetic energy, the horizontal displacement of the seed is shorter during separation. So, it is easy to fall into the effective area of the seed guide mechanism, and the seed delivery performance is better.

3.1.3. Influence of IACB and IADC on the Separation Method

As shown in Figure 9a, the seeds at position B failed to fall into the seed-guiding mechanism at 3.94 s. The seeds left the edge of the dibbler cover and fell inside the seed-guiding mechanism, during which the seeds moved at A in two main separation modes: A_1 for contact separation, and A_2 for noncontact separation, as shown in Figure 9b. Most of the seeds were in the A_1 attitude to B_1 attitude, and a few seeds were fed at the seed-suction tray hole with a certain initial velocity. After bouncing and tumbling along the edge of the dibbler cover, the seeds entered the seed-guiding mechanism in the A_2 attitude due to the collision with the baffle of the seed separation tray during the falling process so that they gained a certain acceleration; if they did not accurately fall into the corresponding area of the seed channel, this resulted in the B_2 attitude at the B position. On the contrary, the seeds fell into the seed-guiding mechanism with A_1 under the push of the baffle of the seed separation tray, and their velocity changes were more stable and trajectories more similar, which thus indicates that the separation of the seeds and seeding disc stopper in the contact state have good seed-feeding advantages.

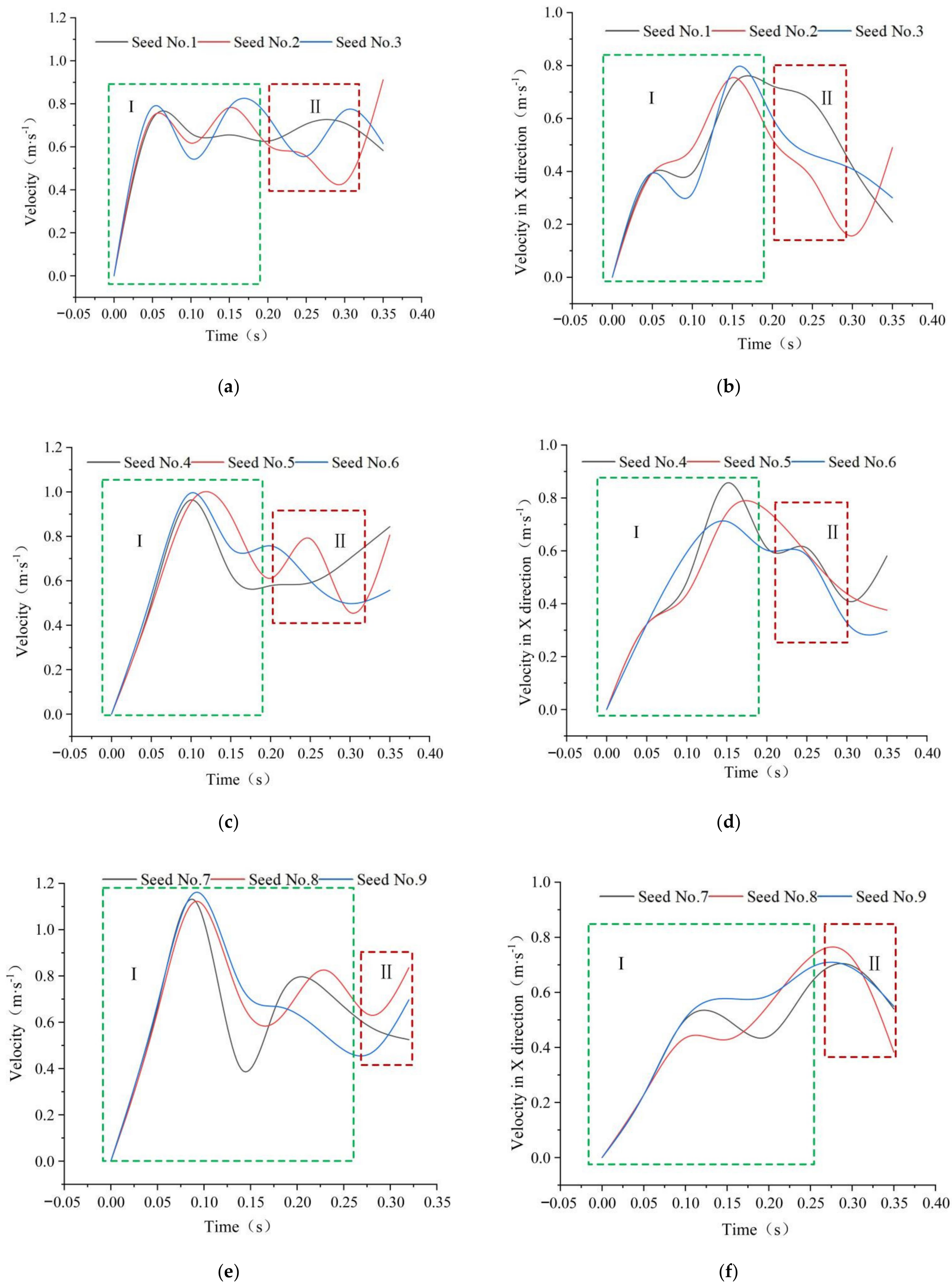

Figure 8. The seed-velocity profile (**a**) 30°;(**c**) 45°;(**e**) 60°; The velocity profile in the *X*-axis direction of the seeds (**b**) 30°;(**d**) 45°;(**f**) 60°.

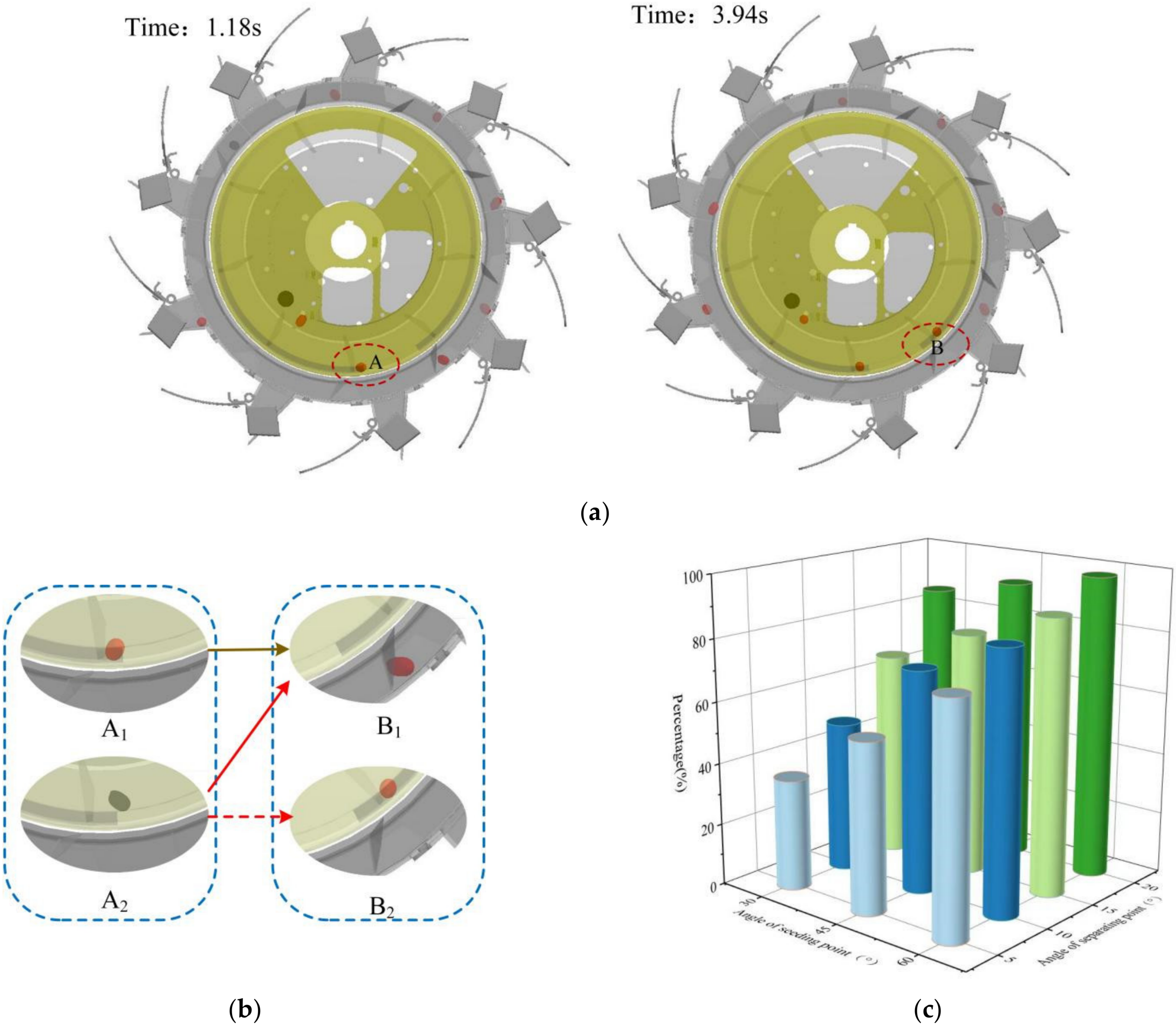

Figure 9. (**a**) Seed distributions at different moments: (**b**) effects of different separation methods; (**c**) effects of different IACB and IADC on contact separation.

We present the percentages of the separation method by A_1 for the different IACB and IADC in Figure 9c. At a certain IADC, the probability of contact separation is $30° < 45° < 60°$, and at a certain IACB, the probability of contact separation is $10° < 15° < 20°$, which shows that, as the IACB and IADC increase, the separation mode of A_1 increases. This law provides ideas for finding the best trajectory for seed feeding.

As the angle between the direction of the force of the baffle on the seed and the horizontal direction gradually increases, the pressure of the seed on the surface of the baffle also increases, which makes the separation process more tends to contact separation. Therefore, increasing the IADC reduces the initial kinetic energy of seed separation and helps maintain the contact between the seed and the baffle, which improves the stability of the seeding process.

3.2. Bench Test Results

We performed multiple-regression fitting analysis on the test data in this study using Design-Expert 10.0.4 software. We present the results of the test indexes corresponding to each test factor for the 17 groups of bench tests in Table 3. According to a preliminary analysis of the test index results, the seeding performance of the dibbler varied under different conditions, with the seeding pass rate distributed between 88% and 96%, the missed seeding rate distributed between 2% and 7%, and the reseeding rate distributed between 1% and 6%.

Table 3. Test factors and indicators.

Serial Number	X_1	X_2	X_3	Seeding Pass Rate (y_1/%)	Missed Seeding Rate (y_2/%)	Reseeding Rate (y_3/%)
1	45	15	4	95.15	3.21	1.64
2	45	15	4	94.43	2.67	2.9
3	45	15	4	95.32	2.89	1.79
4	60	15	5	91.38	4.89	3.73
5	45	10	5	92.72	4.41	2.87
6	45	20	3	91.52	4.57	3.91
7	30	15	5	88.35	6.13	5.52
8	60	20	4	91.81	4.22	3.97
9	30	20	4	88.26	6.21	5.53
10	30	10	4	91.67	4.6	3.73
11	45	15	4	94.84	2.34	2.82
12	45	15	4	94.37	3.11	2.52
13	60	15	3	92.62	4.08	3.3
14	45	20	5	90.29	5.27	4.73
15	30	15	3	89.43	5.93	4.64
16	45	10	3	93.86	3.09	3.05
17	60	10	4	93.17	3.49	3.34

We present the analyses of variance (ANOVA) of the experimental data in Tables 4–6. X_1, X_2, and X_3 had significant effects ($p < 0.01$) on the seeding pass rate, missed seeding rate, and reseeding rate, respectively. The main order of the test indicators was X_1, X_2, and X_3, and the interaction of X_1 and X_2 also had significant effects on the seeding pass rate. The regression-equation misfit terms for the test data's three indicators were insignificant ($p > 0.05$), indicating the test data fit well.

Table 4. ANOVA of seeding pass rate.

Variance Source	Sum of Squares (SS)	Freedom	F	p
Model	81.39	9	71.51	<0.0001
X_1	15.88	1	125.53	<0.0001
X_2	11.38	1	89.95	<0.0001
X_3	2.75	1	21.74	0.0023
X_1X_2	1.05	1	8.31	0.0236
X_1X_3	0.006	1	0.051	0.8284
X_2X_3	0.002	1	0.016	0.9029
X_1^2	28.98	1	229.14	<0.0001
X_2^2	3.97	1	31.39	0.0008
X_3^2	12.95	1	102.37	<0.0001
Residual	0.89	7		
Misfit	0.17	3	0.32	0.8117
Error	0.71	4		
Summation	82.28	16		

Note: $p < 0.01$ means the difference is very significant, and $p < 0.05$ means the difference is significant.

Table 5. ANOVA of missed seeding rate.

Variance Source	SS	Freedom	*F*	*p*
Model	23.53	9	29.59	<0.0001
X_1	4.79	1	54.19	0.0002
X_2	2.74	1	30.98	0.0008
X_3	1.15	1	12.99	0.0087
X_1X_2	0.19	1	2.19	0.1824
X_1X_3	0.093	1	1.05	0.3391
X_2X_3	0.096	1	1.09	0.3317
${X_1}^2$	7.72	1	87.38	<0.0001
${X_2}^2$	0.78	1	8.88	0.0205
${X_3}^2$	4.72	1	53.46	0.0002
Residual	0.62	7		
Misfit	0.13	3	0.35	0.795
Error	0.49	4		
Summation	24.15	16		

Note: $p < 0.01$ means the difference is very significant, and $p < 0.05$ means the difference is significant.

Table 6. ANOVA of reseeding rate.

Variance Source	SS	Freedom	*F*	*p*
Model	18.72	9	9.05	0.0042
X_1	3.23	1	14.03	0.0072
X_2	3.32	1	14.42	0.0067
X_3	0.48	1	2.07	0.1936
X_1X_2	0.34	1	1.49	0.262
X_1X_3	0.051	1	0.22	0.6532
X_2X_3	0.25	1	1.09	0.3317
${X_1}^2$	6.4	1	27.84	0.0012
${X_2}^2$	1.39	1	6.07	0.0433
${X_3}^2$	2.25	1	9.77	0.0167
Residual	1.61	7		
Misfit	0.24	3	0.23	0.8684
Error	1.37	4		
Summation	20.33	16		

Note: $p < 0.01$ means the difference is very significant, and $p < 0.05$ means the difference is significant.

To ensure that all the factors reached significant or highly significant levels, we excluded the effects of interaction factors with $p > 0.1$. We established the regression equations between the seeding pass rate (y_1), missed seeding rate (y_2), and reseeding rate (y_3), and we present the test factors in Equations (11), (12) and (13), respectively:

$$\begin{aligned} y_1 = 94.82 + 1.41X_1 - 1.19X_2 - 0.59X_3 + \\ 0.51X_1X_2 - 2.62{X_1}^2 - 0.97{X_2}^2 - 1.75{X_3}^2 \end{aligned} \tag{11}$$

$$\begin{aligned} y_2 = 2.84 - 0.77X_1 + 0.58X_2 + 0.38X_3 + \\ 1.35{X_1}^2 + 0.43{X_2}^2 + 1.07{X_3}^2 \end{aligned} \tag{12}$$

$$\begin{aligned} y_3 = 2.33 - 0.64X_1 + 0.64X_2 + 1.23{X_1}^2 + \\ 0.58{X_2}^2 + 0.73{X_3}^2 \end{aligned} \tag{13}$$

To visualize the effect of the interaction between the factors on the seeding performance of the dibbler, we generated the response surface between the seeding pass rate and test factors with the Design-Expert 10.0.4 software. The interaction between X_1 and X_2 significantly affects the seeding pass rate (Figure 10). Due to the change in X_2, the direction of the speed of the seed leaving the dibbler cover changes, and the trajectory of the seeds entering the seed-guiding mechanism also changes. When X_1 is constant, the seeding pass rate increases first and then decreases with the increasing X_2. When X_2 is fixed and X_1 increases, the time required for the seed separation from the dibbler cover is gradual, leading to an increasing and then decreasing seed-sowing rate. Therefore, different combinations of X_1 and X_2 can be used to change the seeding trajectory to achieve the desired seed-feeding effect.

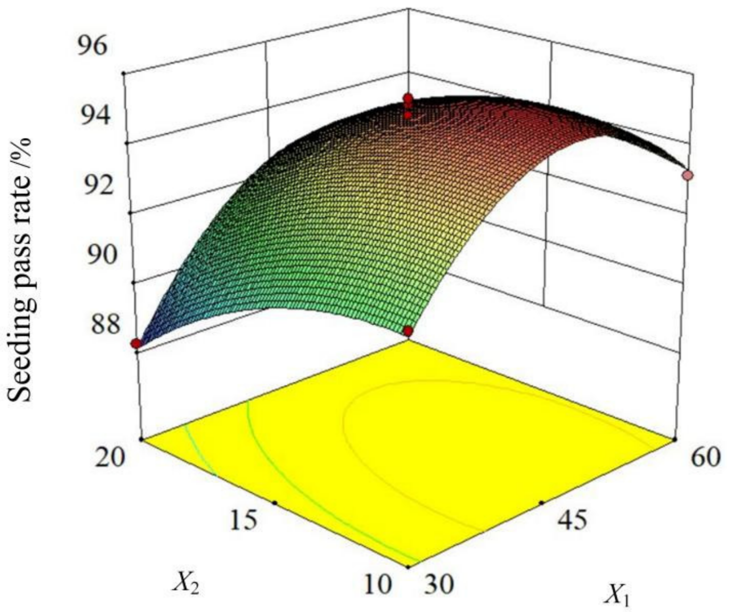

Figure 10. Effect of interaction factors on seeding pass rate.

With the multiobjective-optimization analysis function of Design-Expert software, we optimized the IACB and IADC, as well as the forward speed, with the objectives of lower missed seeding and reseeding indexes and a higher passing index:

$$\begin{cases} \max Y_1 \\ \min Y_2 \\ \min Y_3 \\ s.t. \begin{cases} 30^\circ \le X_1 \le 60^\circ \\ 10^\circ \le X_2 \le 20^\circ \\ 3\text{km}\cdot\text{h}^{-1} \le X_3 \le 5\text{km}\cdot\text{h}^{-1} \end{cases} \end{cases} \tag{14}$$

We calculated that when X_1 was 48.28°, X_2 was 12.29°, and X_3 was 3.84 km·h^{-1}, which are the optimal results that appeared for the parameter combination, where the seeding pass rate was 95.35%, the missed seeding rate was 2.52%, and the reseeding rate was 2.11%.

3.3. Field Trials Results

We present the field test in Figure 11. Driven by a tractor of 70 hp or more, we rounded off the optimized parameter combination by setting the IACB to 48°, the IADC to 12°, and the tractor's forward speed to 3.9 km·h^{-1}. Due to the field machine test in the ground conditions, the machine's vibrations, and other effects, the seeding pass rate slightly decreased, but it was above 92%. The average seeding pass rate was 93.8%. The missed seeding and reseeding rates were low, and the mean rates of missed seeding and reseeding were 3.6% and 2.6%, respectively. The operating performance substantially improved, meeting the peanut single-grain precision-seeding requirements. This further demonstrates the research value of the optimization results.

(a) (b)

Figure 11. (**a**) Field trial verification; (**b**) seeding on film.

3.4. Discussion

(1) For the seed separation from the dibbler-cover phase, the baffle of the seed separation tray pushes the seeds forward. As the angle between the direction of the baffle and the horizontal direction gradually increases, the pressure of the seeds on the surface of the baffle of the seed separation tray also increases, which makes the process more inclined to contact separation;

(2) According to the simulation analysis, the collision between the seeds and the baffle of the seed separation tray is the main reason for reducing the feeding performance of the dibbler in the noncontact separation process. The vibration caused by the unstable ground conditions during the operation of the machine increases the numbers of the noncontact separation method. Thus, we can improve the seeding performance by adjusting the IACB and IADC to find a stable and reliable seed-feeding trajectory;

(3) Previously, the research on the performance of air-suction dibbler was mainly focused on the seed suction performance, but the research on the seed feeding process was relatively rare. When a few researchers studied the seed feeding performance, the optimization method was mainly to improve the structural form of the seed-guiding mechanism to make the seeds move smoothly. There was no experiment on the seed feeding from the seed tray to the seed-guiding mechanism. The technology of smooth and orderly seed feeding under high-speed operating conditions is of great significance in improving the performance of the seed releaser and realizing precision sowing operation.

4. Conclusions

(1) To address the problem of the seeds not accurately falling into the seed-guiding mechanism during the seed-feeding process of the air-suction roller dibbler for peanuts, we propose a method to optimize the seeding trajectory. To determine the IACB, we established a kinetic model to analyze the seed separation from the dibbler-cover phase and their entry into the seed-guiding mechanism;

(2) We performed a single-factor simulation test of the dibbler design with different IACB and IADC using EDEM software. We obtained the influences of the IACB and IADC on the seed-delivery performance. At a certain IADC, the probability of contact separation is $30° < 45° < 60°$; at a certain IACB, the probability of contact separation is $10° < 15° < 20°$, which shows that, as the IACB and IADC increase, so does the separation mode of A_1;

(3) We obtained the best combination of the seeding-performance parameters through a three-factor and three-level combination seeding bench test. We obtained the best seed-feeding performance in the bench test at 48.28° for IACB, 12.29° for the IADC, and 3.84 $km \cdot h^{-1}$ for the machine. The seeding pass rate was 95.35%, the missed seeding rate was 2.52%, and the reseeding rate was 2.11%. The field verification test showed that the

machine worked well with the combination, and the seeding pass rate was above 92%. This meets the requirements of the single-grain precision sowing of peanuts, and the operation performance was substantially improved.

Author Contributions: Conceptualization, Y.X. and J.K.; methodology, Y.X. and J.K.; software, C.Z.; validation, Q.P.; formal analysis, N.Z.; investigation, X.W.; resources, J.K. and C.Z.; data curation, Y.X.; writing—original draft preparation, Y.X.; writing—review and editing, Y.X.; supervision, J.K.; project administration, Y.X.; funding acquisition, J.K. All authors have read and agreed to the published version of the manuscript.

Funding: This research was funded by the National Key Research and Development Program of China, NO. 2020YFD1000902.

Institutional Review Board Statement: Not applicable.

Informed Consent Statement: Not applicable.

Data Availability Statement: Not applicable.

Conflicts of Interest: The authors declare no conflict of interest.

References

1. Zhang, L.; Wang, L. Development status, existing problems and policy recommendations of peanut industry in China. *Trans. CSAE* **2020**, *45*, 116–122.
2. Sun, T.; Li, G.; Ning, T.; Zhang, Z.; Mi, Q.; Rattan, L. Suitability of mulching with biodegradable film to moderate soil temperature and moisture and to increase photosynthesis and yield in peanut. *Agric. Water Manag.* **2018**, *208*, 214–223. [CrossRef]
3. Wan, S.; Zhang, J.; Zhang, Z. A major change in peanut planting technology: Single seed precision sowing. *Trans. Chin. J. Oil Crops* **2020**, *42*, 927–933.
4. Chen, X.; Lu, Y. Sowing performance of Air-suction Cylindrical Cotton Precision Dibbler. *Trans. Chin. Soc. Agric. Mach.* **2010**, *41*, 35–38.
5. Chen, H.; Li, T.; Wang, H.; Wang, Y.; Wang, X. Design and parameter optimization of pneumatic cylinder ridge three-row close-planting seed-metering device for soybean. *Trans. CASE* **2018**, *34*, 16–24.
6. Liao, Y.; Li, C.; Liao, Q.; Wang, L. Research Progress of Seed Guiding Technology and Device of Planter. *Trans. Chin. Soc. Agric. Mach.* **2020**, *51*, 1–14.
7. Yang, L.; Yan, B.; Zhang, D.; Zhang, T.; Wang, Y.; Cui, T. Research Progress on Precision Planting Technology of Maize. *Trans. Chin. Soc. Agric. Mach.* **2016**, *47*, 38–48.
8. Liao, Q.; Deng, Z.; Huang, H. Application of the high speed photography checking the precision metering performances. *Trans. J. Huazhong Agric. Univ.* **2004**, *22*, 570–573.
9. Yu, J.; Ding, Y.; Liao, Y.; Cong, J.; Liao, Q. High-speed photography analysis of dropping trajectory on pneumatic metering device for rapeseed. *Trans. J. Huazhong Agric. Univ.* **2014**, *33*, 103–108.
10. Liu, H.; Xu, X.; Liu, J.; Wang, C. Working characteristics of vertical shallow-basin type seed-metering device based on high-speed photography and virtual simulation. *Trans. CSAE* **2016**, *32*, 13–19.
11. Li, F.; Chen, J.; Liu, F.; Liu, Y.; Zhang, T.; Zhao, M. lnfluence of seed adsorption posture on seeding performance based on high speed camera technology. *Trans. J. China Agric. Univ.* **2018**, *23*, 128–136.
12. Sauder, D. Plattner. U.S. Patent 7152540B1, 26 December 2006.
13. Kocher, M.; Coleman, J.; Smith, J.; Kachman, D. Corn seed spacing uniformity as affected by seed tube condition. *Appl. Eng. Agric.* **2011**, *27*, 177–183. [CrossRef]
14. Ding, L.; Yang, L.; Zhang, D.; Cui, T.; Zhang, L.; Zhong, X. Effect of Seed Adsorption Posture of Corn Air-suction Metering Device on Seed Feeding Performance. *Trans. Chin. Soc. Agric. Mach.* **2021**, *52*, 40–50.
15. Wang, Y.; Zhang, W.; Yan, W.; Qi, B. Design and Experiment of Seed Pressing Device for Precision Seeder Based on Air Flow Assisted Seed Delivery. *Trans. Chin. Soc. Agric. Mach.* **2020**, *51*, 69–76.
16. Lv, J.; Yang, Y.; Shang, Q.; Li, Z.; Li, J.; Li, Z.; Wang, Z.; Wang, Y. Performance Optimization Test on Air-suction Potato Seed Metering Device with Positive Pressure Airflow and Zero-speed Seeding. *Trans. CASE* **2016**, *32*, 40–48.
17. Gao, X.; Zhou, J.; Lai, Q. Design and experiment of pneumatic cylinder precision seed-metering device for panax notoginseng. *Trans. CASE* **2016**, *32*, 20–28.
18. Yang, W.; Kan, C.; Zhang, X.; Wu, C.; Du, Q.; Pan, W. Design and Test of Precision Seed Metering Device for Panax notoginseng Seedling and Seeding by Air Suction. *Trans. Chin. Soc. Agric. Mach.* **2021**, *52*, 95–105.
19. Li, Y.; Yang, L.; Zhang, D.; Cui, T.; Zhang, K.; Jie, C.; Yang, R. Analysis and test of linear seeding process of maize high speed precision metering device with air suction. *Trans. CASE* **2020**, *36*, 26–35.
20. Chen, X.; Zhong, L. Design and test on belt-type seed delivery of air-suction metering device. *Trans. CASE* **2012**, *28*, 8–15.

21. Kang, J.; Wen, H.; Wang, S.; Yan, L. Experimental study on impact of belt type conductor delivery on seeding uniformity. *Trans. China J. Agric. Mach. Chem.* **2015**, *36*, 42–45.
22. Zhang, C.; Kang, J.; Peng, Q.; Zhang, N.; Wang, X.; Jian, S. Design and Test of Secondary Seed Feeding Mechanism of Air-suction Roller Dibbler for Cotton. *Trans. Chin. Soc. Agric. Mach.* **2021**, *52*, 106–116.
23. Tong, C. Zero speed seeding technology and its theoretical design. *Trans. Mech. Res. Appl.* **1995**, *1*, 16–18.
24. Zhao, S.; Chen, J.; Wang, J.; Chen, J.; Yang, C.; Yang, Y. Design and Experiment on V-groove Dialing Round Type Guiding-seed Device. *Trans. Chin. Soc. Agric. Mach.* **2018**, *49*, 146–158.
25. Wang, F.; Lv, B.; Wang, H.; Zhao, M. Structural design and test of seed-suction hole ofair-sucking seed-metering device for millet. *Trans. CASE* **2017**, *33*, 30–36.
26. Wu, M.; Cong, J.; Yan, Q.; Zhu, T.; Peng, X.; Wang, Y. Calibration and experiments for discrete element simulation parameters of peanut seed particles. *Trans. CASE* **2020**, *36*, 30–38.
27. *GB/T 6973-2005*; Single (Precise) Test Method. National Standards of the People's Republic of China: Beijing, China, 2005.
28. Xing, H.; Zang, Y.; Cao, X.; Wang, Z.; Luo, X.; Zeng, S.; Huang, S. Experiment and analysis of dropping trajectory on rice pneumatic metering device. *Trans. CASE* **2015**, *31*, 23–30.
29. Chen, Y.; Sun, X.; Luo, X.; Chen, X.; Li, M.; Li, Y. Design and dynamic balance analysis of cutter roller of vine-cutting machine. *Trans. China J. Agric. Mach. Chem.* **2015**, *36*, 15–17.